Oxidized LDL attenuates apoptosis in monocytic cells by activating ERK signaling

Dmitry Namgaladze, Andreas Kollas, and Bernhard Brüne[1]

Faculty of Medicine, Institute of Biochemistry I, Johann Wolfgang Goethe University, 60590 Frankfurt, Germany

Abstract Low concentrations of oxidized low density lipoprotein (OxLDL) are cytoprotective for phagocytes, although the underlying mechanisms remain unclear. We investigated signaling pathways used by OxLDL to attenuate apoptosis in monocytic cells. OxLDL at 25–50 μg/ml inhibited staurosporine-induced apoptosis in THP-1 cells and mouse peritoneal macrophages, and it was cytoprotective in human primary monocytes upon serum withdrawal. Attenuated cell demise was reversed by blocking extracellular signal-regulated kinase (ERK) signaling. Translocation of cytochrome c to the cytosol was attenuated by OxLDL, which again demanded ERK signaling. Analysis of Bcl-2 family proteins revealed phosphorylation of Bad at serine 112 as well as ERK-dependent inhibition of Mcl-1 degradation. Although the formation of reactive oxygen species (ROS) is an established signal generated by OxLDL, ROS scavengers did not interfere with cell protection by OxLDL.▪ Thus, activation of the ERK signaling pathway by OxLDL is important to protect phagocytes from apoptosis.—Namgaladze, D., A. Kollas, and B. Brüne. **Oxidized LDL attenuates apoptosis in monocytic cells by activating ERK signaling.** *J. Lipid Res.* **2008. 49: 58–65.**

Supplementary key words atherosclerosis • oxidized low density lipoprotein • reactive oxygen species • extracellular signal-regulated kinase

Atherosclerotic plaque progression involves dynamic changes in cellular composition. These changes comprise the migration of cells from the bloodstream into the intima, their egress into the lymph system, and the proliferation and migration of smooth muscle cells from the media. Moreover, cell death affects cell numbers in atherosclerotic plaques. Several studies have established that phagocyte cell death diminished lesion progression during early stages of atherosclerosis (1, 2), whereas an increased death of phagocytes and smooth muscle may contribute to plaque destabilization in advanced atherosclerosis (3, 4).

Modified lipoproteins are important factors in lesion development, and the oxidation of lipoproteins is a characteristic feature of the plaque (5). Oxidized low density lipoproteins (OxLDLs) affect numerous phagocyte functions, including cell survival (6). Although high concentrations of OxLDL are cytotoxic for cells of the vascular wall, cytoprotective actions of OxLDL have been reported at lower doses in phagocytes (7, 8). Recent studies suggest that cytoprotection by OxLDL depends on the degree of its oxidative modification as well as OxLDL inclusion in immune complexes (9, 10).

Mechanistically, OxLDL-evoked cytoprotection was linked to activation of the phosphatidylinositol 3-kinase (PI3K)-Akt survival pathway (7, 9–11). However, little is known regarding other potential antiapoptotic mechanisms conveyed by OxLDL. Activation of extracellular signal-regulated kinase (ERK) constitutes a major mitogenic and antiapoptotic pathway activated by a variety of extracellular agonists, such as growth factors or hormones (12). ERK targets a number of apoptotic regulators, including proteins of the Bcl-2 family (13–15), caspases (16), and inhibitor of apoptosis proteins (17). Although some data suggest that ERK inhibition reduces the viability of OxLDL-treated phagocytes (18), other studies reported ERK not to be involved (7). Therefore, the role of ERK signaling in provoking antiapoptotic actions of OxLDL remains unclear.

In this study, we explored signaling mechanisms evoked by OxLDL in protecting THP-1 monocytic cells from staurosporine-induced cell death. The antiapoptotic effect of OxLDL involved the activation of ERK, whereas PI3K/Akt activation was not involved. Inhibition of apoptosis occurred upstream of cytochrome c trans-

---

location, involved Bad phosphorylation, and impaired Mcl-1 degradation.

MATERIALS AND METHODS

Materials

Cell culture medium and supplements were from PAA Laboratories (Coelbe, Germany). A protein assay kit was from Bio-Rad (Munich, Germany). Protease inhibitors came from Roche Diagnostics (Mannheim, Germany). Nitrocellulose membrane, the ECL detection system, and horseradish peroxidase-labeled anti-mouse and anti-rabbit secondary antibodies were from GE Healthcare (Munich, Germany). N-acetyl-L-aspartyl-L-glutamyl-L-valyl-L-aspartyl (7-amino-4-methylcoumarin) (Ac-DEVD-AMC), LY294002, and PD98059 were from Alexis (Lausen, Switzerland). API2 was from EMD Biosciences (Darmstadt, Germany). All other chemicals were from Sigma (Taufkirchen, Germany). Primary antibodies against phospho-Akt serine 473 (9271), total Akt (9272), phospho-ERK threonine 183/185 (9101), total ERK (9102), phospho-Bad serine 112 (9296), phospho-Bad serine 136 (9295), Bim (4582), Mcl-1 (4572), and caspase-3 (9662) were from Cell Signaling Technology (Beverly, MA). Primary antibodies against Bcl-2 (610539), Bcl-xL (610212), and cytochrome c (556433) were from BD Biosciences (Heidelberg, Germany). Dr. Herman Schaegger (Johann Wolfgang Goethe University, Frankfurt, Germany) kindly provided antibody against ATP synthase (mitochondrial complex V).

LDL isolation and treatment

Human LDL (d = 1.02–1.06 g/ml) was isolated from plasma of healthy volunteers (DRK-Blutspendedienst Baden-Württemberg-Hessen, Institut für Transfusionsmedizin und Immunhämatologie Frankfurt am Main, Frankfurt, Germany) by sequential ultracentrifugation. OxLDL was prepared by incubating LDL with 5 µM $CuSO_4$ at room temperature for 24 h followed by dialysis against PBS with 100 µM EDTA. Oxidation was monitored by measuring the relative electrophoretic mobility of LDL and OxLDL in agarose gels (Lipidophor; Technoclone, Vienna, Austria) as well as by spectrophotometric detection of thiobarbituric acid-reactive substances (TBARS). Our OxLDL preparations showed a relative electrophoretic mobility of 3–4 and 6–8 nmol/mg TBARS. Endotoxin content of the preparations was <1 ng/mg OxLDL (Pyrotell assay; Associates of Cape Cod, Falmouth, MA). Oxidized 1-palmitoyl-2-arachidonoyl-sn-glycero-3-phosphorylcholine (OxPAPC) was prepared as described (19) and was kindly provided by Dr. Valery Bochkov (Medical University of Vienna, Austria).

Cell culture

THP-1 monocytic cells were maintained in RPMI 1640 medium containing 100 U/ml penicillin, 100 µg/ml streptomycin, and 10% heat-inactivated fetal calf serum. Before the experiments, the medium was changed to fetal calf serum-free medium. Human monocytes were isolated from buffy coats (DRK-Blutspendedienst Baden-Württemberg-Hessen, Institut für Transfusionsmedizin und Immunhämatologie Frankfurt am Main) using Ficoll density centrifugation (LSM 1077; PAA Laboratories) followed by magnetic separation with positive selection (CD14 MicroBeads; Miltenyi Biotec, Bergisch Gladbach, Germany). The purity of monocytes was assessed by flow cytometry using CD14 staining. Resident mouse peritoneal macrophages were obtained from C3H/HeJ mice and cultured in RPMI 1640 medium containing 100 U/ml penicillin, 100 µg/ml streptomycin, and 10% heat-inactivated fetal calf serum. Cells were incubated overnight in the same medium without serum before treatments. This study conformed with the principles outlined in the Declaration of Helsinki.

Western blot analysis

Cells were incubated overnight in serum-free medium, treated, collected, lysed in 200 µl of buffer A (50 mM Tris, 150 mM NaCl, 5 mM EDTA, 0.5% Nonidet P-40, 10 mM NaF, 1 mM Na_3VO_4, 1 mM PMSF, and protease inhibitor mixture, pH 7.5), and sonified, followed by centrifugation (15,000 g, 10 min). A total of 30–60 µg of protein was loaded onto and resolved on SDS-polyacrylamide gels. Proteins were blotted onto nitrocellulose. Membranes were blocked and incubated with primary antibodies according to the manufacturer's instructions. Membranes were washed three times for 5 min each with TTBS (10 mM Tris, 150 mM NaCl, and 0.05% Tween 20, pH 7.5). For protein detection, blots were incubated with a horseradish peroxidase-labeled secondary antibody for 1 h and washed three times for 5 min each with TTBS, followed by ECL detection.

Cell death detection

Cells were incubated overnight in serum-free medium, treated, and processed for cell death detection by flow cytometry (FACS Canto; BD Biosciences, Heidelberg, Germany) using the Annexin V-FITC apoptosis detection kit (Beckman Coulter, Krefeld, Germany) according to the manufacturer's instructions. Apoptosis of mouse peritoneal macrophages was assessed by detecting cytoplasmic histone-associated DNA fragments using the cell death ELISA kit from Roche Diagnostics, according to the manufacturer's instructions.

Caspase activity assay

Caspase-3/7 activity was quantified fluorimetrically by following the cleavage of Ac-DEVD-AMC. Cell pellets were resuspended in lysis buffer (100 mM HEPES, pH 7.5, 10% sucrose, 0.1% CHAPS, and 1 mM PMSF), sonified, and centrifuged (10,000 g, 10 min). Cytosolic protein (30 µg) was incubated with 10 µM Ac-DEVD-AMC in the presence of 10 mM DTT at 30°C. Substrate cleavage and accumulation of AMC were followed fluorimetrically with excitation at 360 nm and emission at 460 nm for 1 h.

Cytochrome c release assay

Cytochrome c translocation to the cytosol was monitored by fractionation of cell lysates according to Leist et al. (20). Cell pellets were resuspended in 100 µl of PBS. A total of 100 µl of digitonin/sucrose solution (0.16 mg/ml digitonin and 500 mM sucrose) was added for 30 s, followed by centrifugation at 10,000 g for 1 min. A total of 50 µg of cytosolic and 25 µg of mitochondrial fractions were analyzed by Western blotting for cytochrome c as well as ATP synthase versus ERK as controls for mitochondrial and cytosolic fractions, respectively.

Reactive oxygen species determination

Reactive oxygen species (ROS) generation in THP-1 cells was analyzed by flow cytometry monitoring the oxidation of 2′,7′-dichlorodihydrofluorescein (DCFH). Cells were loaded with 5 µM DCFH-diacetate for 30 min, pelleted, resuspended in PBS, and treated for 1 h with OxLDL and/or antioxidants followed by flow cytometry.

Statistical analysis

Data are expressed as means ± SEM. Two treatment groups were compared by independent Student's t-tests. Results were considered statistically significant at $P < 0.05$.

RESULTS

To investigate the influence of OxLDL on apoptosis, monocytic THP-1 cells were treated with 0.2 µg/ml staurosporine for 4 h to induce the mitochondrial apoptotic signaling pathway. Cell death was followed by Annexin V/propidium iodide staining and flow cytometry. As shown in **Fig. 1A**, staurosporine provoked massive apoptosis and thus cells became Annexin V-positive but basically remained propidium iodide-negative, indicating that only a small fraction of cells was necrotic. Exposing cells to staurosporine in the presence of 50 µg/ml OxLDL drastically reduced the number of apoptotic cells with minor signs of necrosis. Quantification of Annexin V staining and thus apoptosis is shown in Fig. 1B. Inhibition of

staurosporine-induced apoptosis was prominent already at 12.5 µg/ml OxLDL and reached maximal protection with 50 µg/ml. We noticed that at concentrations of 100 µg/ml and greater, OxLDL induced necrotic cell death (19.2 ± 2.7% Annexin V/propidium iodide double-positive cells after 4 h with 150 µg/ml OxLDL), confirming previous data on OxLDL cytotoxicity (21). Native LDL was protective as well, but ~5-fold higher LDL concentrations were needed to achieve an antiapoptotic effect similar to that of OxLDL.

Staurosporine-induced apoptosis involves the activation of caspases, provoking the cleavage and activation of executioner caspases-3 and -7. To evaluate the impact of OxLDL on caspase-3/7, we measured the cleavage of Ac-DEVD-AMC in lysates of THP-1 cells. As shown in
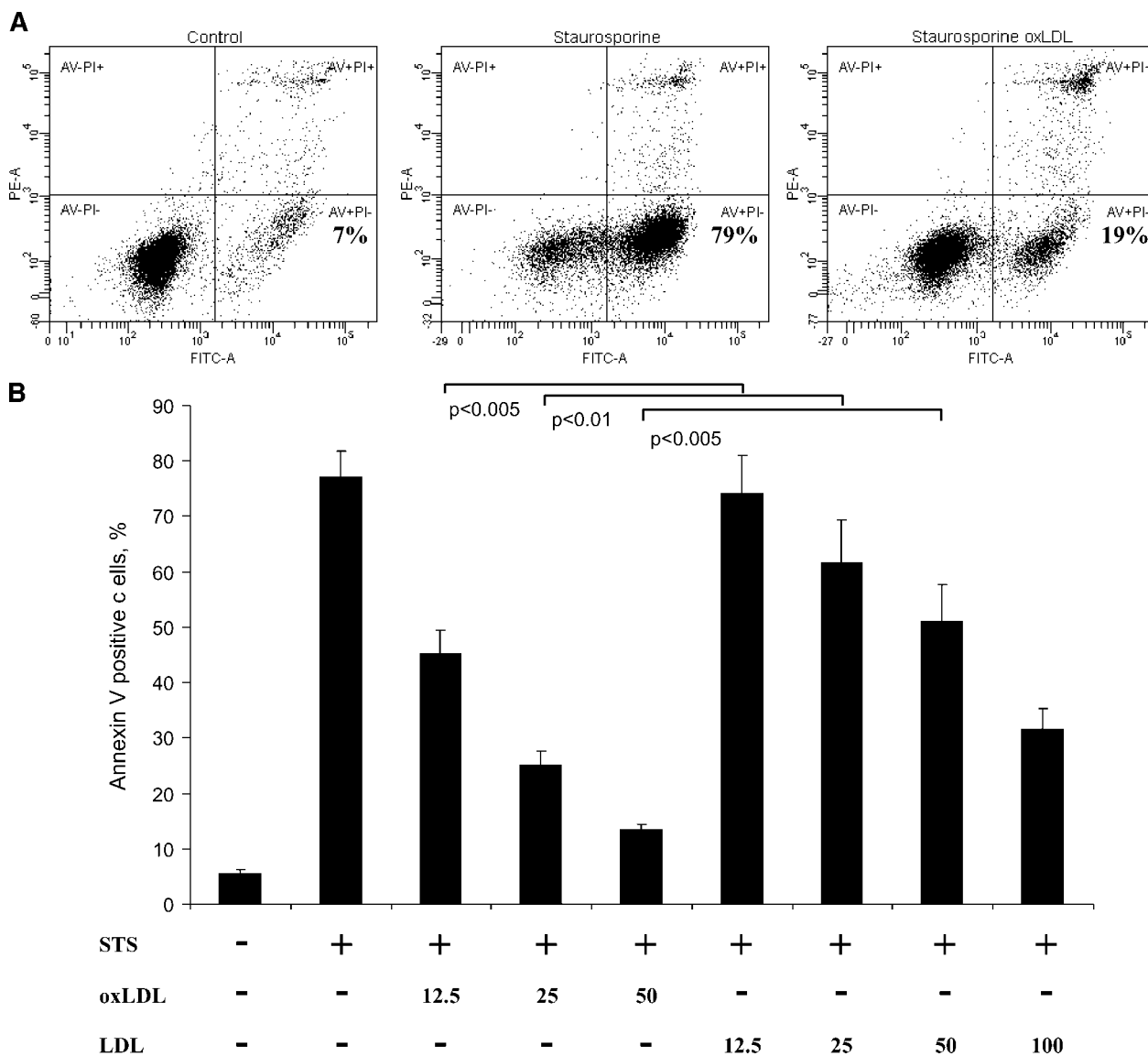

Fig. 1. Oxidized low density lipoprotein (OxLDL) attenuates apoptosis in THP-1 cells. A: Cells were treated with 0.2 µg/ml staurosporine (STS) alone or in combination with 50 µg/ml OxLDL for 4 h, stained with Annexin V/propidium iodide (AV/PI), and analyzed by flow cytometry. Representative dot plot diagrams are shown. Numbers indicate the percentage of Annexin V-positive but propidium iodide-negative cells. B: Cells were treated with 0.2 µg/ml staurosporine alone or in combination with the indicated concentrations of OxLDL or LDL for 4 h. Data are presented as means ± SEM (n > 3). PE-A, phycoerythrin channel fluorescence area.

Fig. 2A, activation of caspase-3/7 by staurosporine was dose-dependently antagonized by OxLDL. Western blot analysis of procaspase-3 and its processed fragments is presented in **Fig. 2B**. Staurosporine induced a time-dependent decrease in the amount of procaspase-3 with a corresponding increase of its cleaved (i.e., 21 and/or 17 kDa) fragments. At 4 h of staurosporine treatment, caspase-3 was cleaved to the 21 kDa fragment, whereas at 8 h, the 17 kDa fragment predominated. Twenty-five as well as 50 µg/ml OxLDL, added together with staurosporine, blocked the processing of procaspase-3 completely, which corroborates caspase activity data.

OxLDL-induced survival of mouse bone marrow-derived macrophages was associated with activation of the PI3K-Akt pathway (7). In addition, activation of mitogen-activated protein kinases, particularly ERK, was linked to growth-promoting and prosurvival actions of OxLDL (18). Therefore, we set out to study these potential prosurvival pathways during protection from apoptosis in THP-1 cells by OxLDL.

In a first set of experiments shown in **Fig. 3A**, we explored the activation of ERK and Akt by OxLDL. OxLDL

Fig. 2. OxLDL diminishes caspase activation by staurosporine. A: Cells were treated with 0.2 µg/ml staurosporine (STS) alone or in combination with the indicated concentrations of OxLDL for 4 h followed by caspase-3/7 activity determinations in cell lysates as described in Materials and Methods. B: Cells were treated with 0.2 µg/ml staurosporine alone or in combination with 25 and 50 µg/ml OxLDL for 4 or 8 h. Cell lysates were subjected to Western analysis to visualize procaspase-3 and cleaved fragments. A representative blot of at least three similar experiments is shown. Data are presented as means ± SEM.

elicited a transient phosphorylation of both Akt and ERK. Maximal effects were seen at 2–10 min, with no changes in the expression of total Akt.

Bad, a proapoptotic Bcl-2 family member, is known to be a target of phosphorylation at serine 112 or serine 136 after activation of ERK or Akt, respectively. OxLDL induced Bad phosphorylation at serine 112 within a time period overlapping with ERK activation (Fig. 3A). However, we could not detect phosphorylation of Bad at serine 136, suggesting that ERK activation dominates for Bad phosphorylation. To further elucidate the role of PI3K-Akt versus ERK signaling in protecting THP-1 cells from apoptosis, we pretreated cells with the PI3K inhibitor wortmannin or blocked mitogen-activated protein kinase kinase with PD98059 before cell stimulation with staurosporine in the presence/absence of OxLDL. As shown for Annexin V staining (Fig. 3B), the protection evoked by OxLDL against staurosporine-induced cell death was reversed by PD98059 but not by wortmannin. Although another PI3K inhibitor, LY294002, reversed cytoprotection by OxLDL, it also reduced OxLDL-induced ERK phosphorylation and thus appeared nonspecific for PI3K/Akt inhibition in our system (data not shown). We also tested inhibitors of two other mitogen-activated protein kinases: SP600125 to block JNK and SB203580 to antagonize p38. Neither of these inhibitors interfered with OxLDL-evoked protection (data not shown).

To explore whether the antiapoptotic effect of OxLDL is not limited only to cell lines, we examined its effect on apoptosis in resident mouse peritoneal macrophages. Apoptosis was assessed by measuring DNA fragmentation using the cell death ELISA kit (Roche Diagnostics). As shown in Fig. 3D, staurosporine treatment of macrophages induced DNA fragmentation, which was reduced significantly in the presence 50 µg/ml OxLDL. Cytoprotection by OxLDL was reversed if cells were preincubated with PD98059. Thus, OxLDL can exert antiapoptotic effects in an ERK-dependent manner in primary macrophages. Additionally, OxLDL increased the viability of human primary monocytes cultured in serum-free medium, a condition known to induce apoptosis in monocytes. Incubations of monocytes with 50 µg/ml OxLDL for 24 h increased cell viability, as measured by the 3-(4,5-dimethylthiazol-2-yl)-2,5-diphenyltetrazolium bromide assay (absorbance at 560 nm = 0.117 ± 0.007 for control and 0.224 ± 0.031 for OxLDL), and reduced caspase-3/7 activity (4,310 ± 1,120 arbitrary units for control and 960 ± 200 arbitrary units for OxLDL).

LDL oxidation generates a diversity of biologically active substances, including oxysterols, lysophospholipids, aldehydes, and oxidized fatty acids. Oxidized phospholipids such as OxPAPC are thought to be generated early in the process of LDL oxidation and represent major components of minimally modified LDL, recently shown to be cytoprotective in macrophages (9). We observed that OxPAPC reduced staurosporine-induced apoptosis of THP-1 cells and that the protection attributed to OxPAPC was partly reversed by PD98059 (Fig. 3C). In contrast, 4-hydroxynonenal
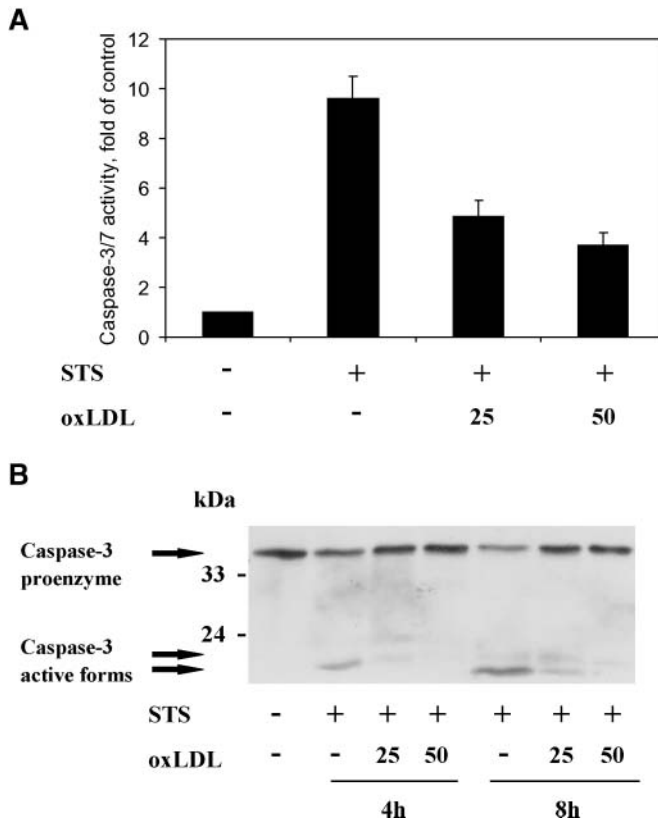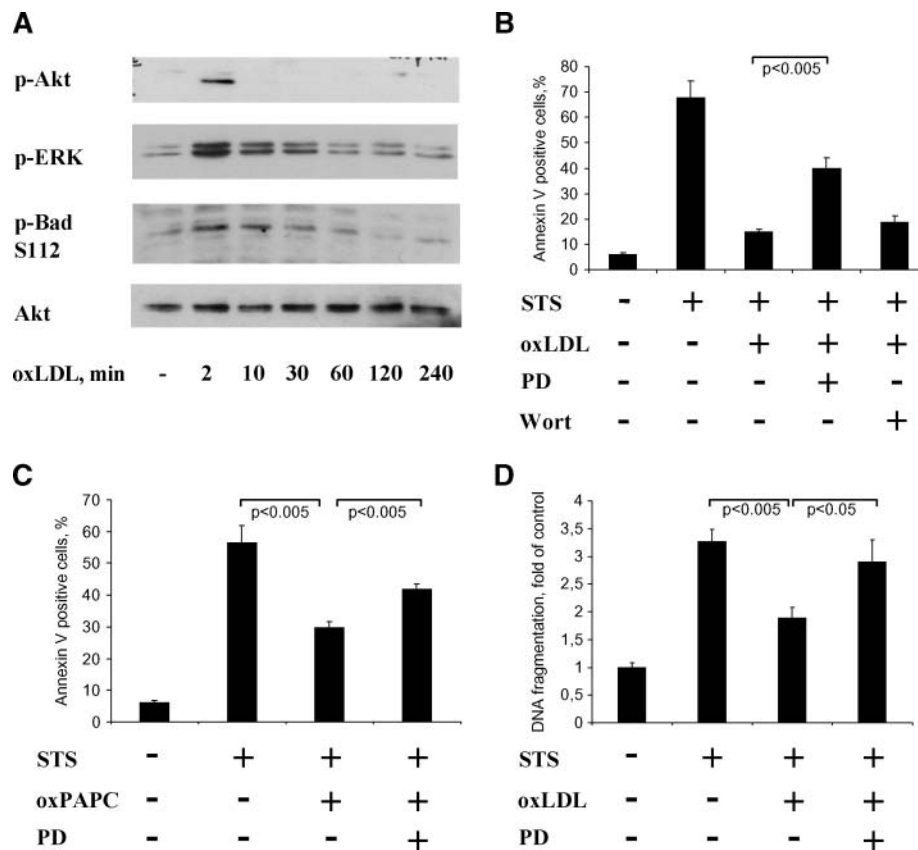
Fig. 3. Role of extracellular signal-regulated kinase (ERK) in the antiapoptotic effects of OxLDL and oxidized phospholipids. A: Cells were treated for the indicated times with 50 μg/ml OxLDL. Cell lysates were subjected to Western analysis using antibodies as described in Materials and Methods. Representative blots of at least three similar experiments are shown. B: Cells were preincubated for 30 min with 100 nM wortmannin (Wort) or 50 μM PD98059 (PD) before incubations with 0.2 μg/ml staurosporine (STS) and/ or 50 μg/ml OxLDL for 4 h. Subsequently, cells were stained with Annexin V/propidium iodide. C: Cells were preincubated for 30 min with 50 μM PD98059 before treatments with 0.2 μg/ml staurosporine and 20 μg/ml oxidized 1-palmitoyl-2-arachidonoyl-*sn*-glycero-3-phosphorylcholine (OxPAPC) for 4 h. Subsequently, cells were stained with Annexin V/propidium iodide. D: Mouse peritoneal macrophages were preincubated for 30 min with 50 μM PD98059 before treatments with 0.02 μg/ml staurosporine and 50 μg/ml OxLDL for 4 h. Subsequently, DNA fragmentation in cell lysates was analyzed by cell death ELISA. All data are presented as means ± SEM (n > 3).

or lysophosphatidylcholine were not cytoprotective under our conditions (data not shown).

Assuming that ERK plays a dominant role in conveying protection by OxLDL raised the question regarding its potential targets. Several ERK targets have been identified in regulating mitochondrial pathways of apoptosis, including proteins of the Bcl-2 family, caspases, and inhibitor of apoptosis proteins. Cytochrome *c* translocation from mitochondria to the cytosol constitutes a central role in the intrinsic cell death signaling cascade. Therefore, we explored whether OxLDL interfered with cell death signaling upstream or downstream of cytochrome *c* release. Cell fractionation followed by Western analysis of cytochrome *c* revealed that staurosporine induced cytochrome *c* release to the cytosol compared with controls, an effect antagonized by OxLDL (**Fig. 4A**). The protection afforded by OxLDL with regard to cytochrome *c* translocation was reversed by PD98059, again suggesting the involvement of ERK signaling. At the same time, the general caspase in-

hibitor z-VAD-fmk did not impair the release of cytochrome *c* from mitochondria but blocked staurosporine-induced apoptosis (data not shown). Cytosolic fractions were controlled for equal protein loading by probing the membranes with ERK antibodies, whereas the lack of contamination with the mitochondrial fraction was confirmed using antibodies against ATP synthase (data not shown). Conclusively, OxLDL interfered with staurosporine-induced apoptosis upstream of cytochrome *c* release.

Cytochrome *c* release is controlled by interactions of proapoptotic versus antiapoptotic members of the Bcl-2 protein family. Several of these proteins constitute ERK targets, including Bad, Bim, or Mcl-1. Therefore, we analyzed the expression of several Bcl-2 family members after THP-1 treatments with staurosporine and/or OxLDL (Fig. 4B). Neither staurosporine nor OxLDL changed the amount of Bcl-2, Bcl-xL, or BimEL. In contrast, staurosporine induced a rapid disappearance of Mcl-1, which is known as a key antiapoptotic player in lymphoid and
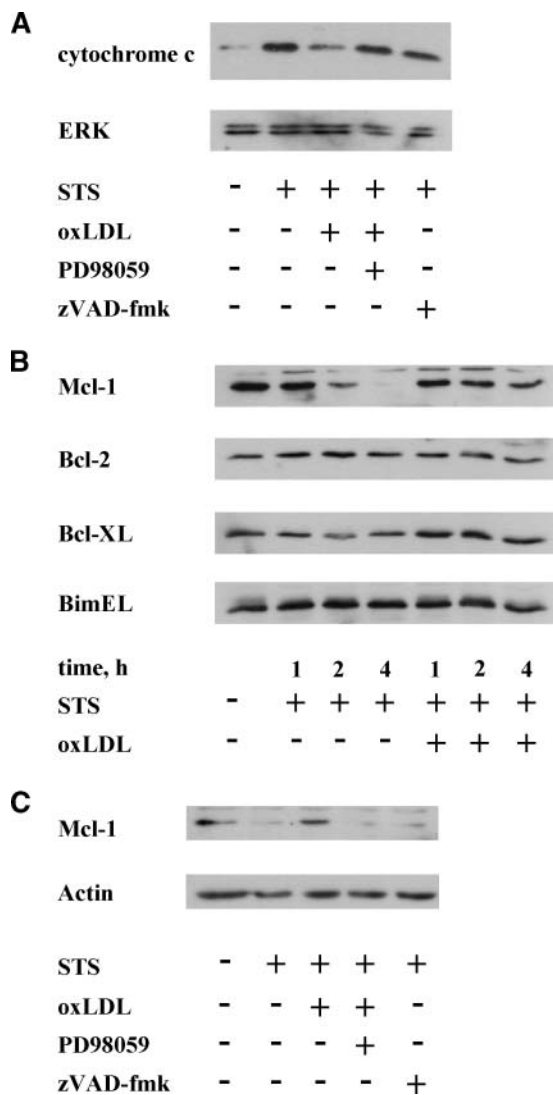
Fig. 4. OxLDL interferes with Mcl-1 degradation after staurosporine treatment. A: Cells were preincubated for 30 min with 50 μM PD98059 or 20 μM zVAD-fmk before treatments with 0.2 μg/ml staurosporine (STS) and/or 50 μg/ml OxLDL for 4 h. Cytochrome *c* release into the cytosol was followed by Western analysis. B: Cells were treated for the times indicated with 0.2 μg/ml staurosporine and 50 μg/ml OxLDL. The protein amount of Bcl-2 family members was assessed by Western analysis. C: Cells were preincubated for 30 min with 50 μM PD98059 or 20 μM zVAD-fmk before the addition of 0.2 μg/ml staurosporine and/or 50 μg/ml OxLDL for 2 h. Mcl-1 levels were analyzed by Western analysis. Representative blots of at least three similar experiments are shown.

myeloid cells. Degradation of Mcl-1 was reduced when staurosporine was supplied in the presence of OxLDL. We went on to investigate whether the attenuation of Mcl-1 degradation by OxLDL was ERK-dependent. As shown in Fig. 4C, the expression of Mcl-1 that was preserved by OxLDL disappeared in the presence of the ERK inhibitor PD98059. Moreover, Mcl-1 degradation was not affected by caspase inhibition, verifying that regulation of Mcl-1 expression is not simply a consequence of reduced apoptosis.

The generation of ROS by OxLDL has been implicated in eliciting several of its biological actions, including cy-

totoxicity (21) and nuclear factor-κB activation (22). Recently, it was suggested that ROS, particularly peroxynitrite, might be involved in OxLDL-induced ERK activation in endothelial cells (23). To determine whether ROS play a role in the inhibition of apoptosis by OxLDL, we measured DCFH oxidation to follow ROS production in OxLDL-treated THP-1 cells. Treatment of THP-1 cells with OxLDL for 1 h increased DCFH oxidation by 3-fold (**Fig. 5A**). DCFH oxidation was reduced significantly in the presence of the peroxyl radical scavenger N,N′-diphenyl-4-phenylenediamine (DPPD) or the lipophylic antioxidant
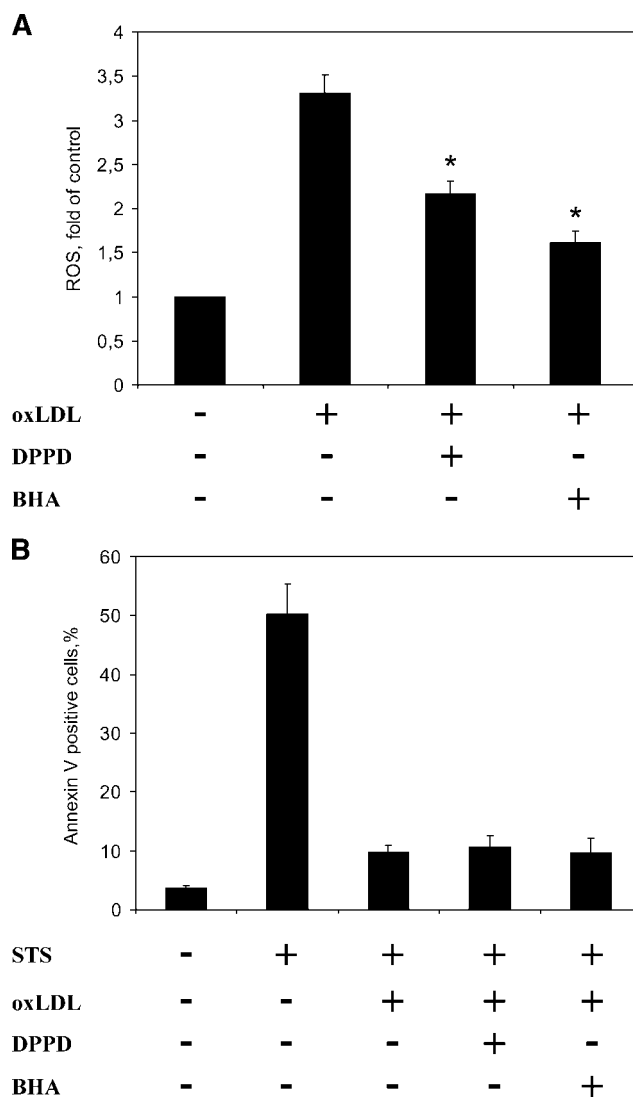

Fig. 5. Reactive oxygen species (ROS) do not transmit the anti-apoptotic action of OxLDL. A: Cells were loaded with 5 μM 2′,7′-dichlorodihydrofluorescein (DCFH)-diacetate for 30 min followed by 1 h treatments with 50 μg/ml OxLDL in the presence or absence of 0.5 μM N,N′-diphenyl-4-phenylenediamine (DPPD) or 50 μM 2[3]-t-butyl-4-hydroxyanisole (BHA), as described in Materials and Methods. DCFH oxidation was monitored by flow cytometry. B: Cells were preincubated for 15 min with 0.5 μM DPPD or 50 μM BHA, followed by a 4 h treatment with 0.2 μg/ml staurosporine (STS) and/or 50 μg/ml OxLDL. Apoptosis was determined by Annexin V/propidium iodide staining. * $P < 0.05$ versus OxLDL (n = 4). Data are presented as means ± SEM.

2[3]-t-butyl-4-hydroxyanisole (BHA). However, neither DPPD nor BHA affected apoptosis inhibition evoked by OxLDL (Fig. 5B), ruling out the possibility that ROS are important for blocking cell death. Interestingly, the same concentrations of DPPD and BHA suppressed toxicity achieved with high OxLDL concentrations (data not shown), thus confirming previous observations showing ROS-dependent OxLDL toxicity to macrophages (21).

DISCUSSION

Our data indicate that active ERK signaling is critical for the suppression of apoptosis by OxLDL in THP-1 cells, thus providing a mechanistic explanation for the antiapoptotic actions of oxidized lipoproteins. Considering that phagocyte apoptosis reduces cell numbers, thereby retarding lesion progression in the early phase of atherosclerosis, suppression of cell death may contribute to the proatherosclerotic actions of OxLDL.

LDL modifications are considered a hallmark during the development of atherosclerosis (5). However, native LDL can also support foam cell formation (24) and activate intracellular signaling pathways (25). We noticed that both OxLDL and native LDL attenuated apoptotic cell death, although the protection by LDL was minor compared with OxLDL. This implies that oxidation confers antiapoptotic properties to LDL. The nature of the OxLDL epitopes responsible for the antiapoptotic action as well as the receptor(s) mediating this effect remain unclear. Recently, it was shown that CD36, a major receptor for OxLDL on phagocytes, transmits only part of the OxLDL signals, with the ERK pathway remaining active in CD36$^{-/-}$ cells (26). Thus, other scavenger receptors, such as LOX-1, may be involved in stimulating ERK (27). Although LDL showed minor protection, the involvement of the LDL receptor can be ruled out. Treatment of LDL with proteinase K did not avert protection induced by LDL, although apoB, the component interacting with the LDL receptor, was lost during proteolytic digestion. Therefore, lipid components of LDL appear more important and lipids such as sphingolipids may contribute to protection (25). In addition, we showed that OxPAPC, an oxidized phospholipid thought to underlie the biological effects of minimally modified LDL, was cytoprotective. Our preparations resulted in LDL being less extensively oxidized compared with the mostly used copper-oxidized LDL. Therefore, oxidized phospholipids may be present in the OxLDL used by us and may be partly responsible for its cytoprotective effect.

We observed potent inhibition of staurosporine-induced phosphatidylserine exposure and caspase activation at 25–50 μg/ml OxLDL. However, at concentrations exceeding 100 μg/ml, OxLDL induced necrosis. A biphasic behavior, with protection dominating at low concentrations but a cytotoxic one at higher doses of OxLDL, is in agreement with published data (7, 8). It is possible that the suppression of apoptotic mechanisms by OxLDL contributes to necrotic cell death at higher OxLDL concentrations and might also be relevant to necrotic core formation in advanced atherosclerosis. Similar observations have been made previously in human macrophages (21), in which OxLDL elicited a caspase-independent but ROS-dependent cell death.

PI3K-Akt and ERK signaling pathways are critical for the regulation of cell survival. We noticed that in addition to antiapoptotic actions attributed to Akt in lipoprotein-induced survival (9, 10, 28), ERK can also be responsible for the cytoprotective effects of OxLDL, as shown by pharmacological inhibition experiments. Previous data and ours imply that both ERK and Akt signaling pathways may be critical for the prosurvival action of modified lipoproteins. Recently, we showed in the same THP-1 system that phospholipase A$_2$-modified LDL activates Akt-dependent survival signaling when cell death was induced by H$_2$O$_2$ or toxic concentrations of OxLDL (28). However, phospholipase A$_2$-modified LDL at concentrations inducing prolonged Akt activation had no effect on staurosporine-induced apoptosis, supporting our notion that Akt activation alone is not sufficient to block staurosporine-induced apoptosis in this system (data not shown). The involvement of ERK signaling in cell protection was recently postulated when inhibition of ERK aggravated 7-ketocholesterol-induced apoptosis (29). As 7-ketocholesterol still induced caspase activation, despite ERK being active, this setup is different from ours, which shows a more prominent impact of ERK in protection.

The release of cytochrome c from mitochondria often is considered the "point of no return" in the cell death execution program. We show that OxLDL inhibits staurosporine-induced cytochrome c release in an ERK-dependent manner. This allows us to conclude that OxLDL interferes early in the apoptotic signaling cascade, most likely involving Bcl-2 family proteins. Indeed, one of the established ERK targets, Bad, was phosphorylated at serine 112, which constitutes the site of phosphorylation by ERK. Additionally, Mcl-1 degradation after staurosporine treatment was reduced by OxLDL, again with ERK inhibition reversing this effect. Mcl-1 is critical for the survival of myeloid cells (30), and interfering with its degradation appears to be an important antiapoptotic signal. Interestingly, BimEL, another ERK target within the Bcl-2 family (13), was not affected, suggesting some specificity in the OxLDL/ERK protective system.

Intracellular ROS generated by OxLDL may participate in initiating various signaling events (31). Along that line, the activation of ERK by OxLDL in endothelial cells involved peroxynitrite-dependent Ras glutathionylation (23). Similarly, lysophosphatidylcholine, an OxLDL constituent, induced ERK activation in endothelial cells, which was dependent on mitochondrial ROS formation (32). Although we observed increased ROS generation by OxLDL that was antioxidant-sensitive, the same inhibitors failed to reverse protection by OxLDL. These results rule out ROS as participating messengers during the antiapoptotic action of OxLDL.

Together, our data provide evidence for the existence of an ERK-dependent antiapoptotic signaling pathway induced by OxLDL in phagocytes. The critical role of ERK

in OxLDL-elicited protection suggests the possibility that blocking this pathway by pharmacological interference would enhance phagocyte apoptosis in the lesion, thus reducing cell numbers and disease progression.▮▮▮

REFERENCES

1. Arai, S., J. M. Shelton, M. Chen, M. N. Bradley, A. Castrillo, A. L. Bookout, P. A. Mak, P. A. Edwards, D. J. Mangelsdorf, P. Tontonoz, et al. 2005. A role for the apoptosis inhibitory factor AIM/Spalpha/ Api6 in atherosclerosis development. *Cell Metab.* **1:** 201–213.

2. Liu, J., D. P. Thewke, Y. R. Su, M. F. Linton, S. Fazio, and M. S. Sinensky. 2005. Reduced macrophage apoptosis is associated with accelerated atherosclerosis in low-density lipoprotein receptor-null mice. *Arterioscler. Thromb. Vasc. Biol.* **25:** 174–179.

3. Tabas, I. 2005. Consequences and therapeutic implications of macrophage apoptosis in atherosclerosis: the importance of lesion stage and phagocytic efficiency. *Arterioscler. Thromb. Vasc. Biol.* **25:** 2255–2264.

4. Clarke, M. C., N. Figg, J. J. Maguire, A. P. Davenport, M. Goddard, T. D. Littlewood, and M. R. Bennett. 2006. Apoptosis of vascular smooth muscle cells induces features of plaque vulnerability in atherosclerosis. *Nat. Med.* **12:** 1075–1080.

5. Lusis, A. J. 2000. Atherosclerosis. *Nature.* **407:** 233–241.

6. Salvayre, R., N. Auge, H. Benoist, and A. Negre-Salvayre. 2002. Oxidized low-density lipoprotein-induced apoptosis. *Biochim. Biophys. Acta.* **1585:** 213–221.

7. Hundal, R. S., B. S. Salh, J. W. Schrader, A. Gomez-Munoz, V. Duronio, and U. P. Steinbrecher. 2001. Oxidized low density lipoprotein inhibits macrophage apoptosis through activation of the PI 3-kinase/PKB pathway. *J. Lipid Res.* **42:** 1483–1491.

8. Hamilton, J. A., G. Whitty, and W. Jessup. 2000. Oxidized LDL can promote human monocyte survival. *Arterioscler. Thromb. Vasc. Biol.* **20:** 2329–2331.

9. Boullier, A., Y. Li, O. Quehenberger, W. Palinski, I. Tabas, J. L. Witztum, and Y. I. Miller. 2006. Minimally oxidized low-density lipoprotein offsets the apoptotic effects of extensively oxidized low-density lipoprotein and free cholesterol in macrophages. *Arterioscler. Thromb. Vasc. Biol.* **26:** 1169–1176.

10. Oksjoki, R., P. T. Kovanen, K. A. Lindstedt, B. Jansson, and M. O. Pentikainen. 2006. OxLDL-IgG immune complexes induce survival of human monocytes. *Arterioscler. Thromb. Vasc. Biol.* **26:** 576–583.

11. Hundal, R. S., A. Gomez-Munoz, J. Y. Kong, B. S. Salh, A. Marotta, V. Duronio, and U. P. Steinbrecher. 2003. Oxidized low density lipoprotein inhibits macrophage apoptosis by blocking ceramide generation, thereby maintaining protein kinase B activation and Bcl-XL levels. *J. Biol. Chem.* **278:** 24399–24408.

12. Ballif, B. A., and J. Blenis. 2001. Molecular mechanisms mediating mammalian mitogen-activated protein kinase (MAPK) kinase (MEK)-MAPK cell survival signals. *Cell Growth Differ.* **12:** 397–408.

13. Ley, R., K. Balmanno, K. Hadfield, C. Weston, and S. J. Cook. 2003. Activation of the ERK1/2 signaling pathway promotes phosphorylation and proteasome-dependent degradation of the BH3-only protein, Bim. *J. Biol. Chem.* **278:** 18811–18816.

14. Scheid, M. P., K. M. Schubert, and V. Duronio. 1999. Regulation of bad phosphorylation and association with Bcl-x(L) by the MAPK/ Erk kinase. *J. Biol. Chem.* **274:** 31108–31113.

15. Derouet, M., L. Thomas, A. Cross, R. J. Moots, and S. W. Edwards. 2004. Granulocyte macrophage colony-stimulating factor signaling and proteasome inhibition delay neutrophil apoptosis by increasing the stability of Mcl-1. *J. Biol. Chem.* **279:** 26915–26921.

16. Allan, L. A., N. Morrice, S. Brady, G. Magee, S. Pathak, and P. R. Clarke. 2003. Inhibition of caspase-9 through phosphorylation at Thr 125 by ERK MAPK. *Nat. Cell Biol.* **5:** 647–654.

17. Gardai, S. J., B. B. Whitlock, Y. Q. Xiao, D. B. Bratton, and P. M. Henson. 2004. Oxidants inhibit ERK/MAPK and prevent its ability to delay neutrophil apoptosis downstream of mitochondrial changes and at the level of XIAP. *J. Biol. Chem.* **279:** 44695–44703.

18. Hamilton, J. A., R. Byrne, W. Jessup, V. Kanagasundaram, and G. Whitty. 2001. Comparison of macrophage responses to oxidized low-density lipoprotein and macrophage colony-stimulating factor (M-CSF or CSF-1). *Biochem. J.* **354:** 179–187.

19. Watson, A. D., N. Leitinger, M. Navab, K. F. Faull, S. Horkko, J. L. Witztum, W. Palinski, D. Schwenke, R. G. Salomon, W. Sha, et al. 1997. Structural identification by mass spectrometry of oxidized phospholipids in minimally oxidized low density lipoprotein that induce monocyte/endothelial interactions and evidence for their presence in vivo. *J. Biol. Chem.* **272:** 13597–13607.

20. Leist, M., C. Volbracht, E. Fava, and P. Nicotera. 1998. 1-Methyl-4-phenylpyridinium induces autocrine excitotoxicity, protease activation, and neuronal apoptosis. *Mol. Pharmacol.* **54:** 789–801.

21. Asmis, R., and J. G. Beagley. 2003. Oxidized LDL promotes peroxide-mediated mitochondrial dysfunction and cell death in human macrophages: a caspase-3-independent pathway. *Circ. Res.* **92:** e20–e29.

22. Cominacini, L., A. F. Pasini, U. Garbin, A. Davoli, M. L. Tosetti, M. Campagnola, A. Rigoni, A. M. Pastorino, V. Lo Cascio, and T. Sawamura. 2000. Oxidized low density lipoprotein (ox-LDL) binding to ox-LDL receptor-1 in endothelial cells induces the activation of NF-kappaB through an increased production of intracellular reactive oxygen species. *J. Biol. Chem.* **275:** 12633–12638.

23. Clavreul, N., M. M. Bachschmid, X. Hou, C. Shi, A. Idrizovic, Y. Ido, D. Pimentel, and R. A. Cohen. 2006. S-Glutathiolation of p21ras by peroxynitrite mediates endothelial insulin resistance caused by oxidized low-density lipoprotein. *Arterioscler. Thromb. Vasc. Biol.* **26:** 2454–2461.

24. Zhao, B., Y. Li, C. Buono, S. W. Waldo, N. L. Jones, M. Mori, and H. S. Kruth. 2006. Constitutive receptor-independent low density lipoprotein uptake and cholesterol accumulation by macrophages differentiated from human monocytes with macrophage-colony-stimulating factor (M-CSF). *J. Biol. Chem.* **281:** 15757–15762.

25. Sachinidis, A., R. Kettenhofen, S. Seewald, I. Gouni-Berthold, U. Schmitz, C. Seul, Y. Ko, and H. Vetter. 1999. Evidence that lipoproteins are carriers of bioactive factors. *Arterioscler. Thromb. Vasc. Biol.* **19:** 2412–2421.

26. Rahaman, S. O., D. J. Lennon, M. Febbraio, E. A. Podrez, S. L. Hazen, and R. L. Silverstein. 2006. A CD36-dependent signaling cascade is necessary for macrophage foam cell formation. *Cell Metab.* **4:** 211–221.

27. Tanigawa, H., S. Miura, Y. Matsuo, M. Fujino, T. Sawamura, and K. Saku. 2006. Dominant-negative lox-1 blocks homodimerization of wild-type lox-1-induced cell proliferation through extracellular signal regulated kinase 1/2 activation. *Hypertension.* **48:** 294–300.

28. Namgaladze, D., and B. Brune. 2006. Phospholipase A2-modified low-density lipoprotein activates the phosphatidylinositol 3-kinase-Akt pathway and increases cell survival in monocytic cells. *Arterioscler. Thromb. Vasc. Biol.* **26:** 2510–2516.

29. Berthier, A., S. Lemaire-Ewing, C. Prunet, T. Montange, A. Vejux, J. P. Pais de Barros, S. Monier, P. Gambert, G. Lizard, and D. Neel. 2005. 7-Ketocholesterol-induced apoptosis. Involvement of several pro-apoptotic but also anti-apoptotic calcium-dependent transduction pathways. *FEBS J.* **272:** 3093–3104.

30. Zhang, B., I. Gojo, and R. G. Fenton. 2002. Myeloid cell factor-1 is a critical survival factor for multiple myeloma. *Blood.* **99:** 1885–1893.

31. Gutierrez, J., S. W. Ballinger, V. M. Darley-Usmar, and A. Landar. 2006. Free radicals, mitochondria, and oxidized lipids: the emerging role in signal transduction in vascular cells. *Circ. Res.* **99:** 924–932.

32. Watanabe, N., J. W. Zmijewski, W. Takabe, M. Umezu-Goto, C. Le Goffe, A. Sekine, A. Landar, A. Watanabe, J. Aoki, H. Arai, et al. 2006. Activation of mitogen-activated protein kinases by lysophosphatidylcholine-induced mitochondrial reactive oxygen species generation in endothelial cells. *Am. J. Pathol.* **168:** 1737–1748.